

# Programmable DNA interstrand crosslinking by alkene-alkyne [2+2] photocycloaddition

Hermann Neitz,<sup>‡</sup> Irene Bessi,<sup>‡</sup> Jochen Kuper,<sup>#</sup> Caroline Kisker,<sup>#</sup> and Claudia Höbartner<sup>†\*</sup>

<sup>‡</sup>Institute of Organic Chemistry Universität Würzburg, Am Hubland, 97074 Würzburg, Germany; <sup>†</sup>Center for Nanosystems Chemistry (CNC), Universität Würzburg, 97074 Würzburg, Germany; <sup>#</sup> Rudolf-Virchow-Zentrum - Center for Integrative and Translational Bioimaging, Universität Würzburg, Josef-Schneider-Straße 2, 97080 Würzburg, Germany.

**ABSTRACT:** Covalent crosslinking of DNA strands provides a useful tool for medical, biochemical and DNA nanotechnology applications. Here we present a light-induced interstrand DNA crosslinking reaction using the modified nucleoside 5-phenylethynyl-2'-deoxyuridine (<sup>Phe</sup>dU). The crosslinking ability of <sup>Phe</sup>dU was programmed by base pairing and by metal ion interaction at the Watson-Crick base pairing site. Rotation to intrahelical positions was favored by hydrophobic stacking and enabled an unexpected photochemical alkene-alkyne [2+2] cycloaddition within the DNA duplex, resulting in efficient formation of a <sup>Phe</sup>dU-dimer after short irradiation times of a few seconds. A <sup>Phe</sup>dU dimer-containing DNA was shown to efficiently bind a helicase complex, but the covalent crosslink completely prevented DNA unwinding, suggesting possible applications in biochemistry or structural biology.

The DNA double helix is an outstanding scaffold for the guided arrangement of functional groups. Precise control of chromophores or reactive groups in DNA can lead to functional materials that offer new opportunities for chemical biology and nanotechnology.<sup>1-4</sup> The formation of a covalent bond between correctly oriented functional groups in single strands leads to the formation of an interstrand crosslink (ICL).<sup>5</sup> ICLs are of interest in biology because they inhibit replication and transcription leading to cellular toxicity.<sup>6</sup> Examples of small molecule-induced ICL are formed by anticancer drugs such as cisplatin<sup>7</sup> or nitrogen mustards.<sup>8</sup> Other common strategies are based on functional groups connected via disulfide<sup>9</sup> or imine formation<sup>10-11</sup>, nucleophilic reactions<sup>12-14</sup> or click reactions.<sup>15-16</sup> Applications aiming at the stabilization of DNA nanostructures<sup>17</sup> often use photochemical reactions that provide an excellent level of control for ICL formation in space and time.<sup>18-23</sup> Prominent examples include classical [2+2] cycloadditions, such as the formation of thymidine dimers,<sup>24-26</sup> fast and reversible photocycloadditions between 3-cyanovinylcarbazole<sup>27-30</sup> or pyranocarbazole<sup>31</sup> with pyrimidine nucleotides, as well as photochemical cyclobutane formation between modified styryl units.<sup>32-33</sup> Crosslinking by [2+2+2] cycloadditions of two alkynes with oxygen was used by Kool et al. for photoswitching of oligodeoxyfluoroside dyes,<sup>34</sup> and by Nagatsugi and coworkers to implement an alkyne-alkyne photocrosslinker using alkyne-modified pyridone groups as nucleobase replacement.<sup>35</sup>

Here, we explored 5-phenylethynyl-2'-deoxyuridine (<sup>Phe</sup>dU, Fig 1A) as building block for programmable DNA interstrand crosslinking. The <sup>Phe</sup>dU nucleoside has previously

been incorporated into DNA to explore its fluorescence response upon hybridization<sup>36</sup> and to modulate electron transport in DNA.<sup>37</sup> Upon photoexcitation of the extended  $\pi$  system we expect different reactivity of the <sup>Phe</sup>dU moiety depending on its orientation in matched or mismatched base pairs (Fig 1B).

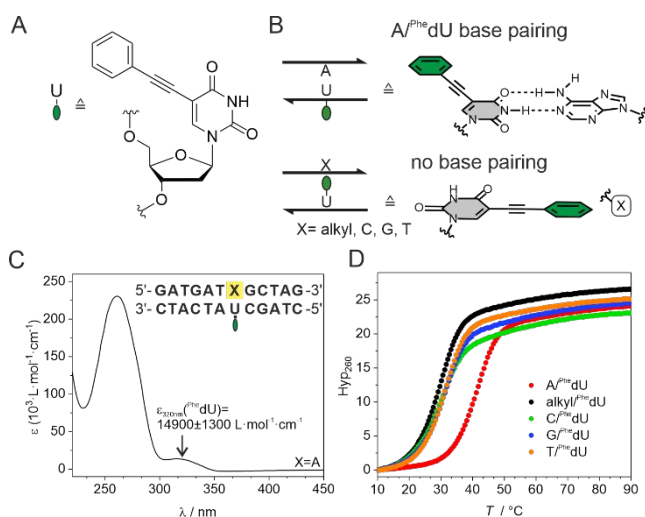


**Figure 1.** (A) Structure of <sup>Phe</sup>dU. (B) Concept of different orientation of <sup>Phe</sup>dU in Watson-Crick base pair (top) versus mismatched situation. (C) UV absorption spectrum of a duplex containing the <sup>Phe</sup>dU modification (X=A). (D) UV melting curves of DNA duplexes containing different nucleobases or an alkyl-nucleobase opposite of <sup>Phe</sup>dU (X=A, C, G, T, or n-propyl), 1  $\mu$ M DNA in sodium phosphate buffer, pH 7.0.

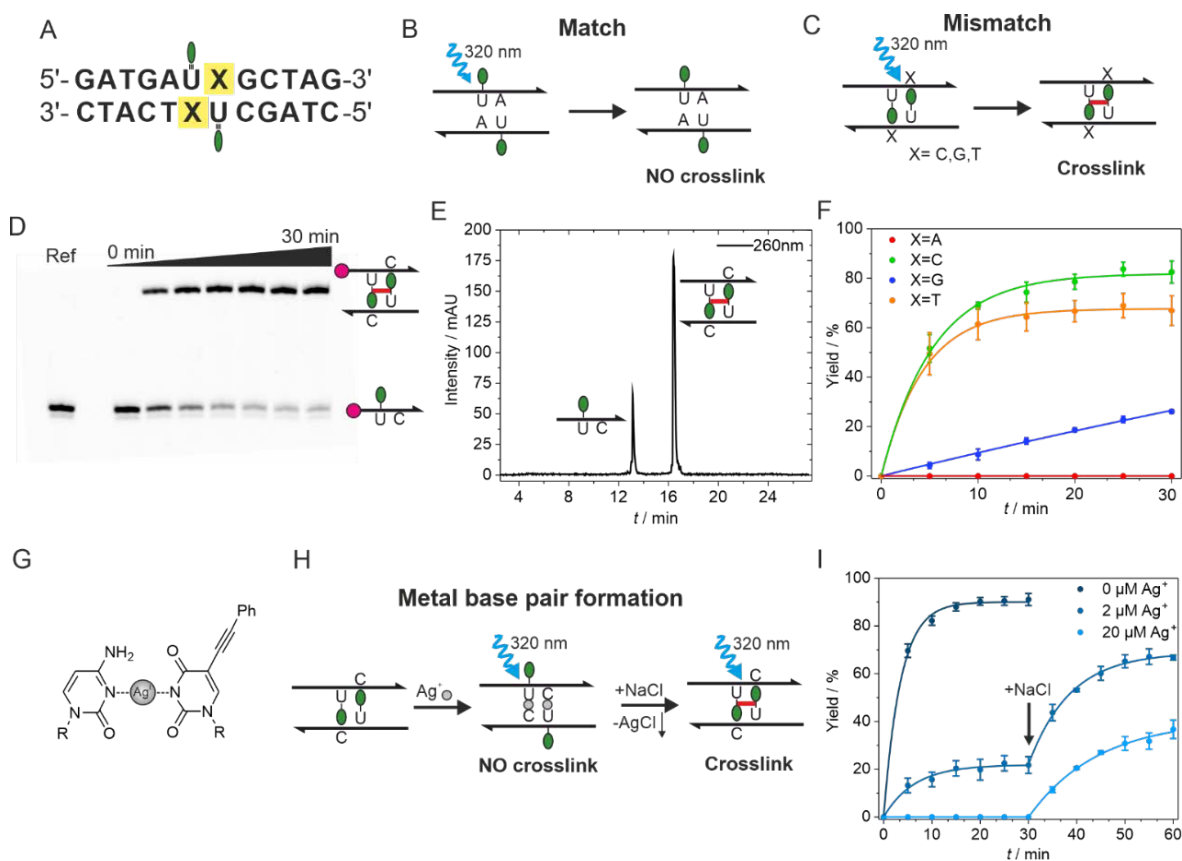


**Figure 2.** (A) DNA duplex used for ICL ( $X=A,C,G,T$ ). Schematic representation of the (B) match ( $X=A$ ) and (C) mismatch ( $X=C,G,T$ ) situation. Exemplary PAGE (D) and anion exchange HPLC (E) analysis of ICL formation with the  $^{\text{Phe}}\text{dU}/\text{dC}$  mismatch. Cy3 is depicted as magenta circle. (F) Kinetics of ICL formation ( $1 \mu\text{M}$  DNA in  $10 \text{ mM}$  sodium phosphate,  $100 \text{ mM}$  NaCl, pH 7.0). (G) Silver-mediated metal base pair between dC and  $^{\text{Phe}}\text{dU}$ . (H) Schematic representation of ICL inhibition by metal base pair formation, and reactivation by precipitation of  $\text{Ag}^+$  as  $\text{AgCl}$ . (I) Kinetics of ICL formation at different  $[\text{Ag}^+]$  ( $1 \mu\text{M}$  DNA in  $10 \text{ mM}$  MOPS,  $100 \text{ mM}$   $\text{NaClO}_4$ , pH 7.1).

The  $^{\text{Phe}}\text{dU}$  nucleoside, which showed a UV absorption maximum at  $306 \text{ nm}$  (Fig S1), was incorporated into DNA oligonucleotides by solid phase synthesis using phosphoramidite chemistry (Scheme S1). The  $^{\text{Phe}}\text{dU}$ -containing duplex showed a UV absorption band at  $320 \text{ nm}$  (Fig 1C, S2). Duplex stability was measured using UV melting curves recorded at  $260 \text{ nm}$ . The base pairing between  $^{\text{Phe}}\text{dU}$  and adenine ( $T_m=40.7 \text{ }^\circ\text{C}$ ) resulted in a slight stabilization compared to the unmodified A/T base pair ( $T_m=40.0 \text{ }^\circ\text{C}$ ). Other nucleotides or an abasic site mimic opposite to  $^{\text{Phe}}\text{dU}$  strongly destabilized the duplex ( $\Delta T_m > 10 \text{ }^\circ\text{C}$ ; Fig 1D).

We designed a duplex containing two  $^{\text{Phe}}\text{dU}$  nucleosides in neighboring base pairs, by placing one  $^{\text{Phe}}\text{dU}$  in each single strand (Fig 2A). Upon formation of Watson-Crick base pairs with adenine ( $X=A$ ), the hydrophobic moieties of the two  $^{\text{Phe}}\text{dU}$  residues point towards the major groove and are located too far apart to undergo any photoreaction with each other (Fig 2B). In contrast, when the Watson-Crick face is not occupied by hydrogen bonding (i.e. in the mismatched situation with  $X=C,G,T$ ), the preferred orientation may be flipped, in order to increase aromatic stacking interactions of the hydrophobic moiety.<sup>38-39</sup> Irradiation with UV light could then result in a photoaddition between the modifications, forming an ICL between the two strands (Fig 2C).

Indeed, we observed ICL formation upon irradiation of the mismatched duplex samples, but not when the Watson-Crick base pair was intact. The kinetics of the crosslink formation was measured by denaturing PAGE using 5'-Cy3-labeled DNA (Fig 2D). In addition, the experiment was performed without a Cy3 fluorophore and analyzed by anion exchange HPLC to show that the crosslinking is independent of the cyanine dye (Fig 2E). Best ICL efficiency was observed when  $^{\text{Phe}}\text{dU}$  was placed in mismatches with pyrimidine nucleotides. The duplex containing  $^{\text{Phe}}\text{dU}$ -deoxycytidine mismatches reached a conversion of about 83% after 30 min of UV irradiation in a stirred quartz fluorescence microcell in a fluorescence spectrometer at  $15 \text{ }^\circ\text{C}$ . The yield for the thymidine  $^{\text{Phe}}\text{dU}$  mismatches was reduced to about 67%, and the  $^{\text{Phe}}\text{dU}$ -dG wobble base pairs gave only 26% ICL (Fig 2F, S3). A transilluminator as light source resulted in faster crosslinking (Fig S4), but the overall ICL yield was lower, likely due to the low  $T_m$  of the double-mismatched 12-mer duplexes (Fig S5). When the duplexes were extended to 20-mers, only 30 s of irradiation on the transilluminator was required to achieve more than 80% ICL yield (Fig S6).

To establish an additional level of control, we turned our attention to metal-ion mediated stabilization of pyrimidine-pyrimidine base pairs.<sup>40</sup> We hypothesized that binding a transition metal between  $^{\text{Phe}}\text{dU}$  and dC or dT would keep the

phenylacetylene group in the major groove and prevent crosslinking, while absence or removal of the metals would favor the reactive stacked orientation. We screened a series of metal ions and examined the crosslinking efficiency by denaturing PAGE (Fig S7). The majority of tested transition metals did not show any effect, but the presence of silver ions clearly inhibited the reaction (Fig 2G-I). The addition of 2  $\mu\text{M}$   $\text{Ag}^+$  to the dC/<sup>Phe</sup>dU sample increased the  $T_m$  by 4.3°C (Fig. S8) and slowed down the crosslink reaction, and 20  $\mu\text{M}$   $\text{Ag}^+$  completely blocked the formation of the ICL. This observation suggests that <sup>Phe</sup>dU undergoes a similar interaction with  $\text{Ag}^+$  as in the known metal base pair of thymidine and cytosine<sup>41</sup>. Upon addition of sodium chloride, the  $\text{Ag}^+$  was removed by precipitation as silver chloride, and the ability to form the ICL was recovered (Fig 2H, S7).

Since the UV-induced reaction between two <sup>Phe</sup>dU was unprecedented, we studied the nature of the crosslinked product in detail. The ICL-containing duplex was isolated in preparative scale and characterized by mass spectrometry and NMR spectroscopy. ESI-MS showed that the irradiated duplex consists of the two <sup>Phe</sup>dU-modified single strands and does not contain any addition of another compound (Fig S9). Considering the previously reported [2+2] cycloaddition of alkyne-modified DNA,<sup>34-35</sup> the incorporation of  $\text{O}_2$  could have been expected, but was not observed. Temperature-dependent NMR spectroscopy of the crosslinked 12mer duplex showed that the ICL provided a thermal stabilization of the duplex, which was also confirmed by UV melting curve analysis of the crosslinked 20mer duplex, which showed a stabilization by 22 °C (Fig S10). The NMR spectra indicated significant signal overlap (Fig S11), which makes assignment of the crosslink resonances challenging and determination of the structure almost impossible. Therefore, the duplex was enzymatically digested and the resulting nucleotide mixture was analyzed by LC/MS. Besides the natural nucleosides dC, dG, dT and dA, two almost co-eluting new products were observed. The extracted ion chromatogram confirmed that both have the same molecular mass, originating from the addition of two <sup>Phe</sup>dU units, without any incorporation of oxygen (Fig 3B, S12). The peak corresponding to the ICL unit was isolated by RP-HPLC and the product was fully characterized. The NMR spectra showed two sets of peaks due to the formation of two isomers. Complete NMR assignment was obtained (Table S3, Fig 3C, S13-15) and the structure determination revealed the formation of a cyclobutene linkage between the <sup>Phe</sup>dU moieties. The photocycloaddition occurred between the C5-C6 double bond of one <sup>Phe</sup>dU and the alkyne of the <sup>Phe</sup>dU unit in the other strand (Fig 3A). The stacking arrangement of the two <sup>Phe</sup>dU units in the duplex places two alkene-alkyne pairs in a symmetrical orientation, which leads to the formation of two diastereomeric <sup>Phe</sup>dU dimers in almost equimolar ratio. The formation of substituted cyclobutenes by photoinduced [2+2] cycloaddition of alkynes and alkenes has been described for various types of activated alkenes with electron-rich alkynes,<sup>42-44</sup> but the reaction has not been observed or used in the context of DNA.

The NMR assignment was fully consistent with the cyclobutene-<sup>Phe</sup>dU dimer formation and the presence of two intact phenyl rings. Nevertheless, other possible cycloaddi-

tions such as photochemical hexadehydro-Diels-Alder reactions<sup>45</sup> or radical cyclization reactions were also considered, which could potentially involve the ortho positions of the phenyl rings. To demonstrate that the phenyl groups

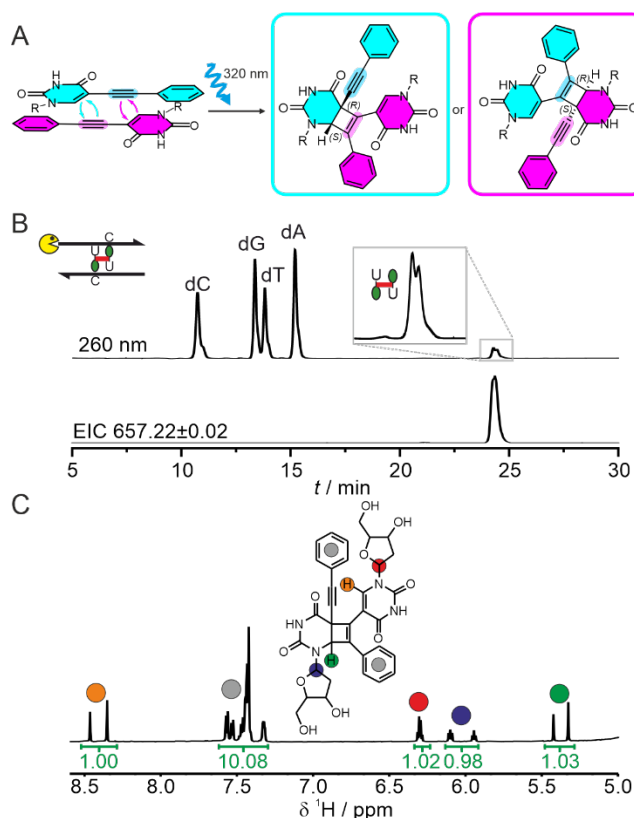


**Figure 3.** (A) <sup>Phe</sup>dU-dimerization by photochemical alkene-alkyne [2+2] cycloaddition. (B) LC/MS analysis of the enzymatically digested DNA duplex containing the ICL. Extracted ion chromatogram (EIC) of <sup>Phe</sup>dU-dimer. (C) Structure of the crosslinked product with assignment of the most relevant protons in the <sup>1</sup>H NMR spectrum (in D<sub>2</sub>O, 600 MHz, 25 °C).

were not directly involved in the crosslink reaction, analogous studies were explored with 5-(pyrimidin-2-yl-ethynyl)-2'-deoxyuridine (<sup>Pym</sup>dU). The corresponding <sup>Pym</sup>dU phosphoramidite was synthesized and incorporated into DNA strands (Scheme S2). The results of the crosslinking reaction with <sup>Pym</sup>dU-modified strands were comparable to the results with <sup>Phe</sup>dU, as observed by PAGE shift and HPLC of the crosslinked duplex, and further confirmed by LC/MS and <sup>1</sup>H-NMR of the <sup>Pym</sup>dU-dimer after digestion (Fig S16). These results showed that the phenyl group is not directly involved in the reaction and can be replaced by another aromatic/heteroaromatic residue that maintains similar hydrophobic interactions and  $\pi$ - $\pi$  stacking geometry. Together with the results of the mixed <sup>Phe</sup>dU/<sup>Pym</sup>dU duplex (Fig S17), these observations support the alkene-alkyne [2+2] photocycloaddition reaction as a plausible mechanism for <sup>Phe</sup>dU and <sup>Pym</sup>dU dimerization as novel type of DNA inter-strand crosslink.

ICLs are DNA damages that prevent unwinding of the DNA duplex and inhibit replication and transcription.<sup>46-47</sup> We expect the <sup>Phe</sup>dU dimer to be recognized as DNA damage and at the same time to act as a roadblock for DNA helicases.

Thus, <sup>Phe</sup>dU could serve as tool for biochemical and biophysical characterization of DNA damage response and DNA repair in vitro. To explore this possibility, we incorporated <sup>Phe</sup>dU into the stem region of an open fork DNA substrate (Y-fork) suitable for helicase assays with 5' to 3' polarity, such as the nucleotide excision repair helicase XPD,<sup>48</sup> and its complex with the structural subunits p44 and p62 of TFIIF.<sup>49-50</sup> The crosslinked version of the Y-fork was formed by UV irradiation (CL Y-fork) (Fig S18), and the PAGE-purified DNA used for analysis of the interaction with proteins. The binding affinity was examined by fluorescence anisotropy and compared to unmodified and <sup>Phe</sup>dU containing DNA Y-forks before crosslinking. All three variants showed similar  $K_D$  values in the nM range (Fig 4A). In addition, formation of the protein-DNA complex was confirmed by an electrophoretic mobility shift assay (Fig 4B, S19). Helicase activity was measured using a fluorophor /quencher system with DABCYL added at the 3' end and Cy3 located at the 5' end of the second strand. After formation of the protein-DNA complexes, helicase activity was initiated by addition of ATP. An increase in Cy3 emission was observed for the unmodified and <sup>Phe</sup>dU containing Y-fork, consistent with unwinding of the duplex by the helicase. In strong contrast, no change in Cy3 emission was detected in the case of the crosslinked Y-fork, indicating effective inhibition of helicase activity (Fig 4C, S20-21). These results demonstrates that the <sup>Phe</sup>dU dimer ICL can be effectively used to lock helicase progression on DNA in vitro.

In summary, we presented a new effective and fast photoinduced interstrand crosslink based on an unexpected alkene-alkyne [2+2] cycloaddition using the known <sup>Phe</sup>dU nucleoside. We demonstrated that the mutual orientation of two <sup>Phe</sup>dU units in a DNA duplex can be switched between inactive and cross-link-competent conformations. The programmability was exploited by Watson-Crick hydrogen bonding or metal-mediated base pairing, in contrast to hydrophobic stacking, to control the DNA crosslink formation. The modified nucleoside is easily accessible and can be precisely incorporated into DNA. Therefore, we expect the new photochemical crosslink to be used for mechanistic and structural studies of DNA-processing enzymes, or for the creation of DNA-based nanostructures.

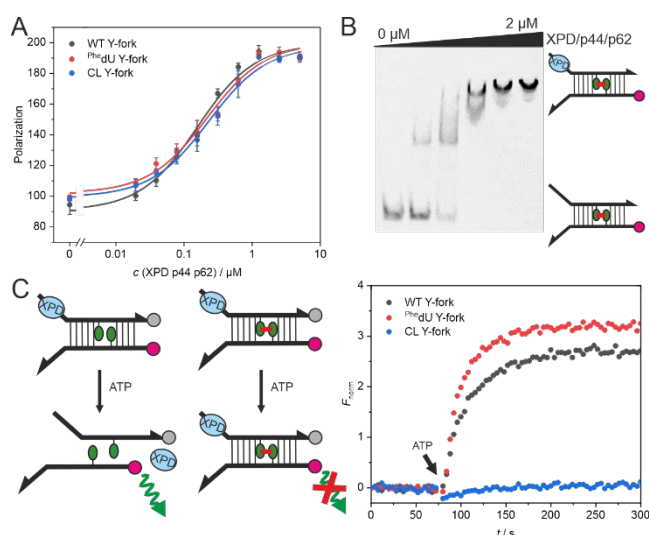


**Figure 4.** (A) Fluorescence anisotropy and (B) electrophoretic

mobility shift assay showing comparable XPD/p44/p62 binding of unmodified and <sup>Phe</sup>dU-containing Y-fork DNA before and after crosslinking. Cy3 label (magenta circle). (C) Helicase assay using Cy3 and DABCYL (gray circle) labeled DNA substrate upon addition of ATP, showing efficient inhibition of unwinding by the crosslinked <sup>Phe</sup>dU-dimer.

## ASSOCIATED CONTENT

**Supporting Information.** Experimental procedures and materials, and additional characterization data by HPLC, mass spectrometry, and NMR spectroscopy. This material is available free of charge via the Internet at <http://pubs.acs.org>.

## Notes

The authors declare no competing financial interest.

## AUTHOR INFORMATION

### Corresponding Author

\*claudia.hoebartner@uni-wuerzburg.de

### ORCID

Hermann Neitz: 0000-0001-9088-5727

Irene Bessi: 0000-0001-9756-1987

Jochen Kuper: 0000-0001-7553-5825

Caroline Kisker: 0000-0002-0216-6026

Claudia Höbartner: 0000-0002-4548-2299

## ACKNOWLEDGMENT

We thank Manuela Michel, Kersten Ulrich and Ricarda Preiss for synthetic contributions and Elke Greiter for providing purified proteins. We acknowledge support by the staff of the mass spectrometry and NMR facilities at the Institute of Organic Chemistry. The University of Würzburg, the Deutsche Forschungsgemeinschaft (DFG) and the European Research Council are gratefully acknowledged.

## REFERENCES

- Seeman, N. C.; Sleiman, H. F., DNA nanotechnology. *Nat Rev Materials* **2017**, *3*, 17068.
- Teo, Y. N.; Kool, E. T., DNA-multichromophore systems. *Chem Rev* **2012**, *112*, 4221-45.
- Micura, R.; Höbartner, C., Fundamental studies of functional nucleic acids: aptamers, riboswitches, ribozymes and DNAzymes. *Chem Soc Rev* **2020**, *49*, 7331-7353.
- O'Reilly, R. K.; Turberfield, A. J.; Wilks, T. R., The Evolution of DNA-Templated Synthesis as a Tool for Materials Discovery. *Acc Chem Res* **2017**, *50*, 2496-2509.
- Onizuka, K.; Yamano, Y.; Abdelhady, A. M.; Nagatsugi, F., Hybridization-specific chemical reactions to create interstrand crosslinking and threaded structures of nucleic acids. *Org Biomol Chem* **2022**, *20*, 4699-4708.
- Schärer, O. D., DNA Interstrand Crosslinks: Natural and Drug-Induced DNA Adducts that Induce Unique Cellular Responses. *ChemBioChem* **2005**, *6*, 27-32.
- Eastman, A., Interstrand crosslinks and sequence specificity in the reaction of cis-dichloro(ethylenediamine)-platinum(II) with DNA. *Biochemistry* **1985**, *24*, 5027-5032.
- Rink, S. M.; Solomon, M. S.; Taylor, M. J.; Rajur, S. B.; McLaughlin, L. W.; Hopkins, P. B., Covalent structure of a nitrogen mustard-induced DNA interstrand cross-link: an N7-to-N7 linkage of deoxyguanosine residues at the duplex sequence 5'-d(GNC). *J Am Chem Soc* **1993**, *115*, 2551-2557.

9. Erlanson, D. A.; Glover, J. N. M.; Verdine, G. L., Disulfide Cross-linking as a Mechanistic Probe for the B ↔ Z Transition in DNA. *J Am Chem Soc* **1997**, *119*, 6927-6928.
10. Tomas-Gamasa, M.; Serdjukow, S.; Su, M.; Muller, M.; Carell, T., "Post-It" Type Connected DNA Created with a Reversible Covalent Cross-Link. *Angew Chem Int Ed* **2015**, *54*, 796-800.
11. Dutta, S.; Chowdhury, G.; Gates, K. S., Interstrand cross-links generated by abasic sites in duplex DNA. *J Am Chem Soc* **2007**, *129*, 1852-3.
12. Kusano, S.; Ishiyama, S.; Lam, S. L.; Mashima, T.; Katahira, M.; Miyamoto, K.; Aida, M.; Nagatsugi, F., Crosslinking reactions of 4-amino-6-oxo-2-vinylpyrimidine with guanine derivatives and structural analysis of the adducts. *Nucleic Acids Res* **2015**, *43*, 7717-30.
13. Peng, X.; Hong, I. S.; Li, H.; Seidman, M. M.; Greenberg, M. M., Interstrand cross-link formation in duplex and triplex DNA by modified pyrimidines. *J Am Chem Soc* **2008**, *130*, 10299-306.
14. Morton, S. B.; Finger, L. D.; van der Sluijs, R.; Mulcrone, W. D.; Hodskinson, M.; Millington, C. L.; Vanhinsbergh, C.; Patel, K. J.; Dickman, M. J.; Knipscheer, P.; Grasby, J. A.; Williams, D. M., Efficient Synthesis of DNA Duplexes Containing Reduced Acetaldehyde Interstrand Cross-Links. *J Am Chem Soc* **2023**, *145*, 953-959.
15. Kocalka, P.; El-Sagheer, A. H.; Brown, T., Rapid and efficient DNA strand cross-linking by click chemistry. *ChemBioChem* **2008**, *9*, 1280-5.
16. Tera, M.; Harati Tajiri, Z.; Luedtke, N. W., Intercalation-enhanced "Click" Crosslinking of DNA. *Angew Chem Int Ed* **2018**, *57*, 15405-15409.
17. Madsen, M.; Gothelf, K. V., Chemistries for DNA Nanotechnology. *Chem Rev* **2019**, *119*, 6384-6458.
18. Lechner, V. M.; Nappi, M.; Deneny, P. J.; Folliet, S.; Chu, J. C. K.; Gaunt, M. J., Visible-Light-Mediated Modification and Manipulation of Biomacromolecules. *Chem Rev* **2022**, *122*, 1752-1829.
19. Qiu, Z.; Lu, L.; Jian, X.; He, C., A diazirine-based nucleoside analogue for efficient DNA interstrand photocross-linking. *J Am Chem Soc* **2008**, *130*, 14398-9.
20. Kobertz, W. R.; Essigmann, J. M., Solid-Phase Synthesis of Oligonucleotides Containing a Site-Specific Psoralen Derivative. *J Am Chem Soc* **1997**, *119*, 5960-5961.
21. Op de Beeck, M.; Madder, A., Sequence specific DNA cross-linking triggered by visible light. *J Am Chem Soc* **2012**, *134*, 10737-40.
22. Rajendran, A.; Endo, M.; Katsuda, Y.; Hidaka, K.; Sugiyama, H., Photo-cross-linking-assisted thermal stability of DNA origami structures and its application for higher-temperature self-assembly. *J Am Chem Soc* **2011**, *133*, 14488-91.
23. Hentschel, S.; Alzeer, J.; Angelov, T.; Scharer, O. D.; Luedtke, N. W., Synthesis of DNA interstrand cross-links using a photocaged nucleobase. *Angew Chem Int Ed* **2012**, *51*, 3466-9.
24. Brown, T. M.; Fakhri, H. H.; Saliba, D.; Asohan, J.; Sleiman, H. F., Stabilization of Functional DNA Structures with Mild Photochemical Methods. *J Am Chem Soc* **2023**, *145*, 2142-2151.
25. Antusch, L.; Gass, N.; Wagenknecht, H. A., Elucidation of the Dexter-Type Energy Transfer in DNA by Thymine-Thymine Dimer Formation Using Photosensitizers as Artificial Nucleosides. *Angew Chem Int Ed* **2017**, *56*, 1385-1389.
26. Gerling, T.; Kube, M.; Kick, B.; Dietz, H., Sequence-programmable covalent bonding of designed DNA assemblies. *Sci Adv* **2018**, *4*, eaau1157.
27. Yoshimura, Y.; Fujimoto, K., Ultrafast reversible photo-cross-linking reaction: toward in situ DNA manipulation. *Org Lett* **2008**, *10*, 3227-30.
28. Fujimoto, K.; Yamada, A.; Yoshimura, Y.; Tsukaguchi, T.; Sakamoto, T., Details of the ultrafast DNA photo-cross-linking reaction of 3-cyanovinylcarbazole nucleoside: cis-trans isomeric effect and the application for SNP-based genotyping. *J Am Chem Soc* **2013**, *135*, 16161-7.
29. Gerling, T.; Dietz, H., Reversible Covalent Stabilization of Stacking Contacts in DNA Assemblies. *Angew Chem Int Ed* **2019**, *58*, 2680-2684.
30. Kishi, J. Y.; Liu, N.; West, E. R.; Sheng, K.; Jordanides, J. J.; Serrata, M.; Cepko, C. L.; Saka, S. K.; Yin, P., Light-Seq: light-directed in situ barcoding of biomolecules in fixed cells and tissues for spatially indexed sequencing. *Nat Methods* **2022**, *19*, 1393-1402.
31. Fujimoto, K.; Sasago, S.; Mihara, J.; Nakamura, S., DNA Photo-cross-linking Using Pyranocarbazole and Visible Light. *Org Lett* **2018**, *20*, 2802-2805.
32. Doi, T.; Kawai, H.; Murayama, K.; Kashida, H.; Asanuma, H., Visible-Light-Triggered Cross-Linking of DNA Duplexes by Reversible [2+2] Photocycloaddition of Styrylpyrene. *Chemistry* **2016**, *22*, 10533-8.
33. Abdelhady, A. M.; Onizuka, K.; Ishida, K.; Yajima, S.; Mano, E.; Nagatsugi, F., Rapid Alkene-Alkene Photo-Cross-Linking on the Base-Flipping-Out Field in Duplex DNA. *J Org Chem* **2022**, *87*, 2267-2276.
34. Chan, K. M.; Kolmel, D. K.; Wang, S.; Kool, E. T., Color-Change Photoswitching of an Alkynylpyrene Excimer Dye. *Angew Chem Int Ed* **2017**, *56*, 6497-6501.
35. Onizuka, K.; Ishida, K.; Mano, E.; Nagatsugi, F., Alkyne-Alkyne Photo-cross-linking on the Flipping-out Field. *Org Lett* **2019**, *21*, 2833-2837.
36. Hudson, R. H.; Ghorbani-Choghamarani, A., Oligodeoxynucleotides incorporating structurally simple 5-alkynyl-2'-deoxyuridines fluorometrically respond to hybridization. *Org Biomol Chem* **2007**, *5*, 1845-8.
37. Tanaka, M.; Oguma, K.; Saito, Y.; Saito, I., Drastic enhancement of excess electron-transfer efficiency through DNA by inserting consecutive 5-phenylethynyl-2'-deoxyuridines as a modulator. *Chem Commun* **2012**, *48*, 9394-6.
38. Neitz, H.; Bessi, I.; Kachler, V.; Michel, M.; Höbartner, C., Tailored Toluene-Perfluorotoluene Assembly as Supramolecular Base Pair Replacement in DNA. *Angew Chem Int Ed* **2023**, *62*, e202214456.
39. Dietzsch, J.; Bialas, D.; Bandorf, J.; Würthner, F.; Höbartner, C., Tuning Exciton Coupling of Merocyanine Nucleoside Dimers by RNA, DNA and GNA Double Helix Conformations. *Angew Chem Int Ed* **2022**, *61*, e202116783.
40. Clever, G. H.; Kaul, C.; Carell, T., DNA--metal base pairs. *Angew Chem Int Ed* **2007**, *46*, 6226-36.
41. Funai, T.; Aotani, M.; Kiriu, R.; Nakamura, J.; Miyazaki, Y.; Nakagawa, O.; Wada, S. I.; Torigoe, H.; Ono, A.; Urata, H., Silver(I)-Ion-Mediated Cytosine-Containing Base Pairs: Metal Ion Specificity for Duplex Stabilization and Susceptibility toward DNA Polymerases. *ChemBioChem* **2020**, *21*, 517-522.
42. Maturi, M. M.; Bach, T., Enantioselective catalysis of the intermolecular [2+2] photocycloaddition between 2-pyridones and acetylenedicarboxylates. *Angew Chem Int Ed* **2014**, *53*, 7661-4.
43. Pappas, S. P.; Pappas, B. C.; Portnoy, N. A., Alkyne-Quinone photoaddition. Synthesis and solvolytic rearrangement of 1-methoxybicyclo[4.2.0]octa-3,7-diene-2,5-dione. *J Org Chem* **1969**, *34*, 520-525.
44. Ha, S.; Lee, Y.; Kwak, Y.; Mishra, A.; Yu, E.; Ryou, B.; Park, C. M., Alkyne-Alkene [2 + 2] cycloaddition based on visible light photocatalysis. *Nat Commun* **2020**, *11*, 2509.
45. Ma, X.; Maier, J.; Wenzel, M.; Friedrich, A.; Steffen, A.; Marder, T. B.; Mitric, R.; Brixner, T., Direct observation of o-benzyne formation in photochemical hexadehydro-Diels-Alder (hnu-HDDA) reactions. *Chem Sci* **2020**, *11*, 9198-9208.
46. Khan, I.; Sommers, J. A.; Brosh, R. M., Jr., Close encounters for the first time: Helicase interactions with DNA damage. *DNA Repair* **2015**, *33*, 43-59.
47. Pandey, M.; Patel, S. S., Helicase and polymerase move together close to the fork junction and copy DNA in one-nucleotide steps. *Cell Rep* **2014**, *6*, 1129-1138.

48. Kuper, J.; Wolski, S. C.; Michels, G.; Kisker, C., Functional and structural studies of the nucleotide excision repair helicase XPD suggest a polarity for DNA translocation. *EMBO J* **2012**, *31*, 494-502.

49. Barnett, J. T.; Kuper, J.; Koelmel, W.; Kisker, C.; Kad, N. M., The TFIIH subunits p44/p62 act as a damage sensor during

nucleotide excision repair. *Nucleic Acids Res* **2020**, *48*, 12689-12696.

50. Petrusseva, I.; Naumenko, N.; Kuper, J.; Anarbaev, R.; Kappenberger, J.; Kisker, C.; Lavrik, O., The Interaction Efficiency of XPD-p44 With Bulky DNA Damages Depends on the Structure of the Damage. *Front Cell Dev Biol* **2021**, *9*, 617160.

## TOC Figure

